Title: Strategic capture of the Nb7 polyoxometalate

Authors: Nicolas Martin; Enric Petrus; Mireia Segado; Ana Arteaga; Lev Zakharov; Carles Bo; May Nyman

To be cited as: 10.1002/chem.201902770

Link to VoR: https://doi.org/10.1002/chem.201902770

Strategic capture of the {Nb_7} polyoxometalate

Nicolas P. Martin[a], Enric Petrus[b], Mireia Segado[b], Ana Arteaga[a], Lev N. Zakharov[a], Carles Bo[b] and May Nyman*[a]

Abstract:

Group V Nb-polyoxometalate (Nb-POM) chemistry generally lacks the elegant pH-controlled speciation exhibited by Group VI (Mo,W) POM chemistry. Here we isolate and structurally characterize three Nb-POM clusters; $[Nb_{14}O_{40}(O_2)_2H_3]^{14-}$, $[((UO_2)(H_2O))_3Nb_{46}(UO_2)_2O_{136}H_8(H_2O)_4]^{24-}$, and $[(Nb_7O_{22}H_2)_4(UO_2)_7(H_2O)_6]^{22-}$, that effectively capture the aqueous Nb-POM species from pH-7 to pH-10. These Nb-POMs illustrate a reaction pathway for control over speciation that is driven by countercations (Li^+) rather than pH. The two reported heterometallic POMs (with UO_2^{2+} moieties) are stabilized by replacing labile H_2O/HO-Nb=O with very stable O=U=O. The third isolated Nb-POM features cis-yl-oxos, prior observed only in group VI POM chemistry. Moreover, with these actinide-heterometal contributions to the burgeuoning Nb-POM family, it now transects all major metal groups of the periodic table.

Polyoxometalates (POMs) are early d^0 transition metal polyanion clusters with wide-ranging applications including catalysis,[1] molecular biology and medicine,[2] energy production and storage,[3] and building blocks for intricate[4] or simple[5] functional materials. Group VI (Mo, W) yields fascinating high nuclearity POMs including {Mo_{368}},[6] {Mo_{248}},[7] {Mo_{176}},[8] {W_{224}},[9] {W_{200}}[10] and {W_{148}}[11] that approach the size of nanoparticles; yet remain molecular in their solubility, absolute formulae and architecture, redefining the 'inorganic molecule'. The rich diversity of size and topologies of these clusters is accessed via pH-control and redox chemistry to promote rearrangement. Such rational synthetic approaches, common to organic chemistry, is rare in aqueous inorganic chemistry where functional groups are labile, and oftentimes transient and unidentified. Such is the case with Group V polyoxoniobates (PONb), mainly confined to alkaline pH, and to date, is completely redox inert. The Lindqvist hexaniobate is the predominant species in aqueous solution above pH-12 and has been used as a precursor for the synthesis of larger compounds by reducing pH, applying hydrothermal conditions, and adding heteroatoms. Several higher nuclearity PONb-clusters were isolated in the last decade by this approach including {Nb_{24}},[12] {Nb_{32}},[12b] {Nb_{52}},[13] {Nb_{81}},[13] {Nb_{114}}[13] and {Nb_{288}}.[14] Most of these are built of either Keggin-derivatives, first isolated in 2002,[15] or from a modified Lindqvist ion; the heptaniobate {Nb_7} (Figure 1). The latter always assembles into larger species, due to the high reactivity of the $Nb(O,OH,OH_2)_3$ appendix-unit on the hexaniobate core. Larger assemblies of the {Nb_7} unit include heterometal clusters with Cu[12a] or Cr[16], and most commonly the {Nb_{24}} stabilized and crystallized with copper amine adducts[12b-d] and recently with europium.[17] Not surprising, the {Nb_7} unit has never been isolated in the solid state without the two of the three above-mentioned terminal O/OH/OH_2-ligands stabilized by polymerization.

Broadly speaking, despite 17 years of expansion of heteropolyniobate chemistry that includes incorporation of first-row transition metals[16, 18] and even acid-stable Nb/Ta-POMs[19], Nb-POM chemistry lacks the rational synthetic approaches that are employed for Group VI POM chemistry. Advances have ensued via hydrothermal processing to obtain higher Nb oxide solubility at lower pH[15], since many studies report 10.5 as close to ideal[12]. Additionally, incorporating open shell transition-metals in Nb-POMs was achieved by rigorous exclusion of alkali countercations that otherwise promote precipitation of these base-insoluble metal oxides. Most syntheses of Nb-POMs featuring the {Nb_7} unit used K-{Nb_6} as starting material. This involves acidification; the mechanism is neither understood nor well-controlled since hydrous niobium oxide precipitates upon acidification of {Nb_6}.

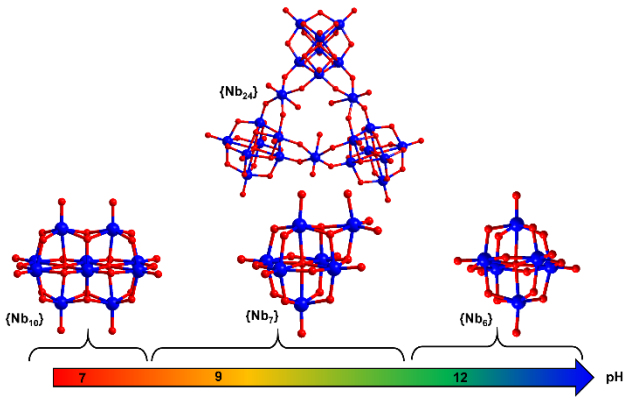

Figure 1. Representation of the most common polyoxoniobates as a function of pH. Left: $[Nb_{10}O_{28}]^{6-}$ unit; top center: $[Nb_{24}O_{72}H_9]^{15-}$ unit; bottom center: $[Nb_7O_{22}]^{9-}$ unit; (right) $[Nb_6O_{19}]^{8-}$ unit. Nb atoms: blue, oxygen atoms: red.

We have recently reported the formation of {Nb_{24}}-sized species in solution[20] simply by mixing tetramethylammonium (TMA) decaniobate $[Nb_{10}O_{28}]^{6-}$, {Nb_{10}} with an alkali salt. This reaction proceeded even if buffered near neutral pH, providing a

[a] Dr. N.P. Martin, Ana Arteaga, Dr. L.N. Zakharov, Dr. M. Nyman
Department of Chemistry
Oregon State University
Gilbert Hall, Corvallis, Oregon 97331, United States
E-mail: may.nyman@oregonstate.edu
[b] E. Petrus, Dr. M. Segado, Dr. C. Bo
Institut Catalá dInvestigació Química (ICIQ), The Barcelona Institute of Science and Technology, Av. Países Catalans, 17, Tarragona, 43007, Spain
[c] Departament de Química Física i Inorgànica. Universitat Rovira i Virgili, Marcel·li Diomingo s/n, Tarragona, 43007, Spain
Supporting information for this article is given via a link at the end of the document.

rare example in which alkali counterions rather than pH drives cluster speciation. Both {Nb_7} and {Nb_{24}} units were identified by electrospray ionization mass spectrometry, while small-angle X-ray scattering (SAXS) showed the {Nb_{24}} units are linked by alkalis. Despite the monodispersity of these solutions evidenced by SAXS, we were never able to obtain crystals for absolute identification of cluster forms. This may be related to the inherent instability of the {Nb_{24}} structure with its three niobyl units with an aqua/hydroxyl ligand trans to the yl-oxo ligand. Therefore we targeted replacing the O=Nb—OH/OH_2 units with the very stable uranyl, O=U=O. We chose $Li_4UO_2(O_2)_3$[21] (noted as Li-U_1) as our uranyl source because 1) it is stable and soluble in mildly alkaline conditions, and 2) the Li can promote disassembly of the {Nb_{10}} cluster, as described in our prior publication[20].

In this synthetic approach, {Nb_{10}} rapidly fragmented, likely accelerated by the peroxide, yielding three structures that effectively captured the {Nb_7} fragment. In polyanion 1, denoted **{$U_3(Nb_{23}U)_2$}**, two {$Nb_{23}U$} units (substitution of a uranyl cation in {Nb_{24}}) are linked to each other by three uranyl monomers. Polyanion 2, **{$U_7(Nb_7)_4$}**, is a supra-tetrahedron of {Nb_7} linked by uranyl. Polyanion 3 does not contain uranyl, and is an {Nb_7} dimer, denoted **{Nb_{14}}**. In **{Nb_{14}}**, the {Nb_7} units mutually link by one of the three terminal oxo-ligand positions of the appendix niobyl, but the other two remain terminal, disordered with peroxide ligands. While cis-terminal oxos are known in Group VI POMs[22], this is the first recognition that this moiety could exist in group V POM chemistry. Computational studies confirmed peroxide-oxo disorder recognized by crystallography is the most stable configuration. Moreover, it showed the cis O=Nb=O is metastable, explaining the ~45% substitution of peroxide at these sites. These first three structures from this synthetic approach illustrate how {Nb_{10}} can be used as a starting material for rational and even strategic Nb-POM synthesis, which has been long-missing from Group V alkaline POM chemistry.

Upon dissolving {Nb_{10}} plus Li-U_1 (details in SI) in water, disassembly of {Nb_{10}} is observed within seconds via Raman spectroscopy with complete disappearance of the 936 cm^{-1} peak, representing the symmetric terminal oxo stretch (Figure S1). Simultaneously, a new peak at 896 cm^{-1} becomes prominent, indicating formation of a distinctly different niobate compound. The peaks located at 853 and 815 cm^{-1} are attributed to peroxo bridges and $U=O_{yl}$ respectively. Vapor diffusion of ethanol into the solution promoted growth of a mixture of crystals including two hybrid niobyl-uranyl compounds: **{$U_3(Nb_{23}U)_2$}** and **{$U_7(Nb_7)_4$}** (crystallographic details reported in table S1). **{$U_3(Nb_{23}U)_2$}** is described as two $Nb_{23}U$ units linked by uranyl cations (Figure 2). This arrangement recalls the {Nb_{24}} dimer linked by alkalis proposed by computational studies in our previous report[20]. A similar dimer has been isolated in the solid state using europium[17]. The three uranyl cations adopt a pentagonal bipyramid geometry with typical $U=O_{yl}$ bond distances (1.761(11)-1.815(8) Å). In the equatorial plane, four oxygen atoms link Nb atoms from two different $Nb_{23}U$ units (U-O = 2.299(8)-2.360(7) Å) plus one terminal water molecule ($U\text{-}O_{aqua}$ = 2.510(8)-2.544(9) Å). The two {$Nb_{23}U$} units are crystallographically independent and are very similar to the well-known {Nb_{24}} cluster, but some niobium monomers linking the {Nb_7} units are disordered with uranyl cations. Single crystal X-ray diffraction reveals four of the six Nb monomers share their positions with uranium atoms with variable occupancies (Table S2) leading to the approximate formula $[((UO_2)(H_2O))_3Nb_{46}(UO_2)_2O_{136}H_8(H_2O)_4]^{24-}$. Details of the disorder are summarized in the SI. Despite the other impurities in the reaction solution, we were able to manually select crystals for several characterizations. EDX measurements revealed an Nb/U ratio of 88.3/11.7 (Figure S8) which corresponds to 6 uranyl and 45 Nb per cluster. Per cluster, 2 TMA counterions, 7 Li cations and 41 water molecules were located by X-ray diffraction. According to the prior-reported Nb_{24} structures[12a, 12d], we can assume each {$Nb_{23}U$} unit can carry at least 8 protons, meaning 8 additional Li are required for charge-balance that could not be located in the lattice, typical of Li-POM salts.[23] Neither the electron density map nor bond valence sum (BVS; **Table S3**) calculations could locate the protons precisely, typical of POM salts, and we therefore assume these are disordered on the oxo ligands of the POMs.

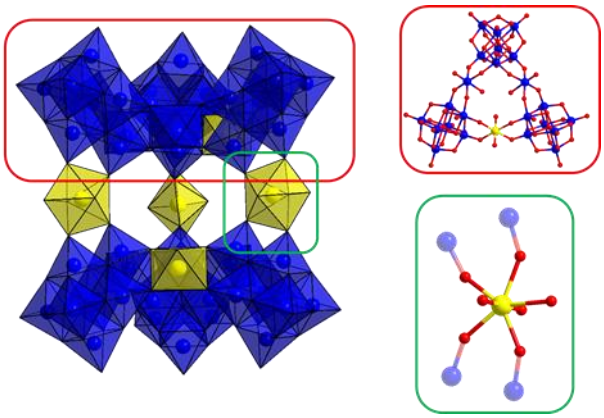

Figure 2. (left) Representation of **{$U_3(Nb_{23}U)_2$}** (right). The {$Nb_{23}U$} unit is circled in red and the central uranyl cation linking the two {$Nb_{23}U$} units is circled in green. Nb: blue, U: yellow, O: red

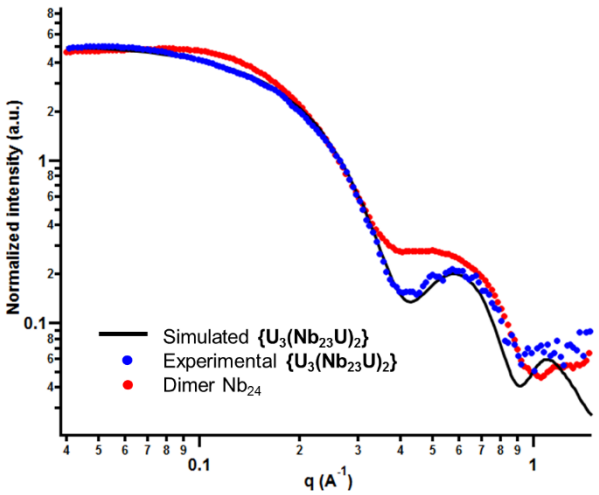

Figure 3. Scattering curve of **{$U_3(Nb_{23}U)_2$}** (blue). Simulated **{$U_3(Nb_{23}U)_2$}** unit (black) and experimental **Nb_{24}** dimer[20] (red).

Small angle X-ray scattering (SAXS) of **{$U_3(Nb_{23}U)_2$}** orange

block crystals redissolved in DI water (Figure 3) shows the experimental scattering matches well with scattering simulated from the X-ray structure. The agreement in the Guinier region (0.09-0.4 $Å^{-1}$) and through the first oscillation (0.4-1 $Å^{-1}$) shows the cluster remains intact in water. We also compared the data with a solution reported prior as a dimer of $\{Nb_{24}\}$ linked by Li^{+}[20]. The two scattering curves are similar meaning the size and the shape of the compounds are comparable. However, **$\{U_3(Nb_{23}U)_2\}$** shows a more pronounced oscillation due to the presence of uranium connecting the two $\{Nb_{24}\}$ units.

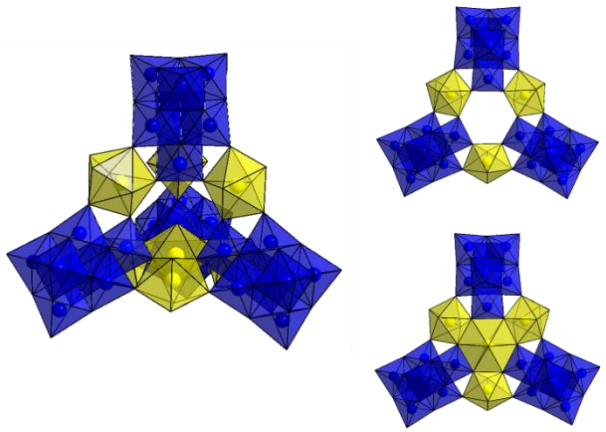

Figure 4. (left) Representation of compound **$\{U_7(Nb_7)_4\}$**. (right) View of the two different types of faces of the supratetrahedron in **$\{U_7(Nb_7)_4\}$**. Top right: view of a face without the central U3 atom (75% occupancy). Bottom right: Central U atom on the face (25% occupancy).

$\{U_7(Nb_7)_4\}$ is described as four $\{Nb_7\}$ units at the apices of a tetrahedral cage (Figure 4). Those units are linked to each other via two independent uranyl atoms (U1 and U2). Both adopt a pentagonal bipyramid geometry (U-O_{yl} = 1.805(14) - 1.817(15) Å; U-ONb = 2.305(10) - 2.396(11) Å; one disordered terminal aqua U-O_{aqua} = 2.49(2) - 2.62(3) Å). This arrangement can be described as interconnected $\{Nb_{24}\}$ units in which uranyl monomers replace Nb monomers. As explained in the SI, this slightly affects the $\{Nb_7\}$ unit configuration and mainly the seventh Nb, compared to those prior-reported $\{Nb_{24}\}$ units.

In the center of each face of the tetrahedron, uranyl and a water molecule are disordered. The uranyl (U3) is 8-coordinate with 25% occupancy, meaning only one is present per molecular unit leading to the formula $[(Nb_7O_{22}H_2)_4(UO_2)_7(H_2O)_6]^{22-}$ (Figure S5). The yl-oxo of this uranyl position in the center of the tetrahedron is common to the four disordered uranium, leading to the long U-O_{yl} bond (1.972(2) Å). The second *–yl* oxygen atom, pointing to the outside, also has an occupancy of 0.25, and the U-O_{yl} bond is 1.69(5) Å. The bond distances between the uranium center and the six oxygen atoms in the equatorial plane are unusually long (2.601(11) - 2.857(12) Å), also likely due to the disorder of this uranyl. Within the $\{Nb_6\}$ unit, the Nb-O_{yl} bond distances are in the typical range 1.744(13) - 1.780(11) Å; but a bit longer (1.792(11) - 1.818(12) Å) for the oxygens bridging to a uranium atom. To charge balance each cluster, only 6 Li and no TMA were located of the required 22 cations. As described above for **$\{U_3(Nb_{23}U)_2\}$**, we can assume 8 protonated oxos on the cluster and 14 Li cations provide the remaining charge-balance. BVS calculations (**Table S4**), similar as described above, could not reveal the positions of charge-balancing protons.

The last compound (**$\{Nb_{14}\}$** Figure 5) crystallizes as colorless square plates (orthorhombic *Pccn*, see SI) from the $\{Nb_{10}\}$-Li-U_1 aqueous mixture following slow evaporation of the solution. The **$\{Nb_{14}\}$** structure provides a unique prospective of the $\{Nb_7\}$ fragment; this is its first isolation as a specie different from $\{Nb_{24}\}$ and without a heterometal.[12-13] The $\{Nb_7\}$ unit (Figure 1) is as described above. Of the three 'terminal' sites of the appendage-Nb (Nb7 in the cif file), two are disordered oxo/peroxide, and the third bridges to the second $\{Nb_7\}$ unit. The Nb=O_{yl} ─Nb bond distance is ~2.0 Å, and the bond angle that bridges the two $\{Nb_7\}$ units is slightly bent at 163°. Prior, an analogue of $\{Nb_{14}\}$ in which Pt with terminal cis-OH ligands located at the Nb7 site was reported.[24]

As mentioned above, Nb7 has two cis terminal groups, disordered between -yl oxo (Nb=O_{yl} = 1.75 and 1.79 Å) and peroxo groups (Nb-O_p = 1.92-1.97 Å), see Figure S7. Free refinement of the occupancy factors of both groups converged to 58% and 55% for –yl oxo and 42% and 45% for the corresponding peroxo; meaning each Nb7 usually has approximately a coordination environment of $NbO_5(O_2)$. Nb has pentagonal bipyramidal coordination with significant distortion in both the equatorial plane and along the O-Nb=O_{yl} axis (Figure S7).

This disorder shows a slight preference toward the cis yl-oxo structures. Since cis Nb=O_{yl} has not been recognized prior, we performed computational studies to determine if is a stable specie, and to help understand the disorder observed by crystallography. Nine isodesmic reactions corresponding to the formation of $\{Nb_{14}\}$ with all possible combinations of peroxo-oxo ligands (Figure S8) were established. For each we determined the relative Gibbs energy and calculated the Boltzmann weight (Table S6). The latter estimates the probability of having an –yl-oxo (56%) or a peroxide (44%) group at each of the four sites, in good agreement with the free occupancy refinement of the X-ray data. The table of Nb-O bond distances and Nb-O=Nb angles of all calculated isomers is reported in the SI and also confirms the configuration described above is fully consistent with X-ray structure. Those calculations also revealed the isomers **2**-iso1 (figure 5) and **2**-iso2 (figure S8) are the major species (61% and 16% respectively) but units presenting cis-yl-oxo group are also stable (22% in total). Note that the difference in stability between peroxide and cis–yl-oxo species is less than 1 kcal·mol^{-1}. Such cis-yl-oxo groups are known for group VI POMs,[22] but this is the first evidence that it is also possible for Group V POM chemistry.

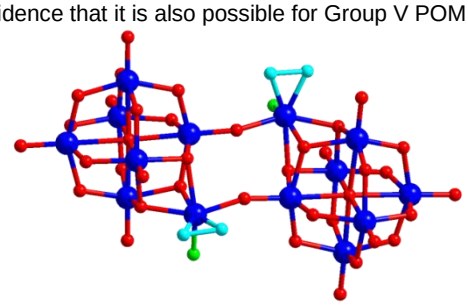

Figure 5. View of the Nb_{14} unit. Nb in blue, O in red, peroxo group in light blue and cis –yl oxo groups in green.

The formula of these dimeric units is $[Nb_{14}O_{40.26}(O_2)_{1.74}]^{14-}$ (according to the X-ray data), which can be approximated as $[Nb_{14}O_{40}(O_2)_2]^{14-}$. To obtain charge-balance, 14 counterions are required but only one TMA molecule and 10 Li atoms have been located by the X-ray data. In this case, it is very reasonable to assume each $\{Nb_{14}\}$ carries three protons; again not precisely located according to BVS calculations (**Table S5**). Four Li-cations and water molecules form a chain and are bridged to the Nb_{14} unit via two more Li (**Figure S7**). The lithium atoms at the end of the chain and the two linked to the terminal oxos of the Nb-POM are in tetrahedral geometry, whereas the two in the center of the Li chain are hexacoordinate. Four other Li atoms, one TMA molecule and 31 water molecules are also observed between the dimeric units. The lithium cations also have regular tetrahedral or octahedral coordination in **{$U_3(Nb_{23}U)_2$}**, in which the O^{2-}-ligands originate exclusively from Nb and U *–yl* groups and bridging oxo-ligands of the POMs. Through this linking, Li-**{$U_3(Nb_{23}U)_2$}** assembles as a 2D framework (**figure S4**). According to Li^+-coordination to both bridging and terminal oxygens of the $\{Nb_7\}$ units of **{$U_3(Nb_{23}U)_2$}** and **{Nb_{14}}**, we recognize basic behavior of **{Nb_7}** is intermediate between that of **{Nb_{10}}** and **{Nb_6}.** Basicity is evidenced by protonation and alkali-bonding in solid-state and in solution: in **{Nb_6}**, the bridging oxygens are more basic, while in **{Nb_{10}},** specific terminal oxygens are more basic.[25]

Strategic substitution of stable UO_2^{2+} for the least stable NbO^{3+} units in prior-reported $\{Nb_{24}\}$ proved fruitful, yielding two intricate heterometal $\{Nb_7\}$-based cluster species. Unexpectedly, the peroxide ligand from the uranyl stabilized a simple Nb_7-dimer without heterometal adducts. This $\{Nb_{14}\}$ cluster provides structural and corroborative computational evidence that the O=Nb=O cis-yl-oxo that has been long known for Group VI POM chemistry is also possible for Group V POM chemistry. All prior-reported solid-state structures of the $\{Nb_7\}$ unit involve a synthetic pathway starting from higher pH species $\{Nb_6\}$. This study follows the opposite pH-trajectory from neutral $\{Nb_{10}\}$ to higher pH. Importantly, a clearer picture of pH control over Nb-POM speciation is emerging that provides opportunity for rational syntheses and applying Nb-POMs as material building blocks[5]. Finally, the few prior examples of hybrid polyoxometalate-actinyl clusters,[26] in addition to the current report, suggest there is rich structural chemistry to be discovered. With this contribution, hybrid Nb-POM chemistry now spans all the metal groups on the periodic table.

Acknowledgements

This study was supported by the U.S. Department of Energy, Office of Basic Energy Sciences, Division of Material Sciences and Engineering, under award DE SC0010802. We thank CBMM, Araxá, Minas Gerais, Brazil for the generous gift of hydrous niobia. The ICIQ researchers thank CERCA Program, ICREA and AGAUR (2017SGR00290) of the Generalitat de Catalunya, and the Spanish Ministerio de Ciencia, Innovación y Universidades through project CTQ2017-88777-R. The OSU researchers gratefully acknowledge the Murdock Charitable Trust (grant # SR-2017297) for acquisition of the single-crystal X-ray diffractometer.

Keywords: Polyoxometalates • uranyl • niobium • polyoxoniobate • heptaniobate

[1] M. Blasco-Ahicart, J. Soriano-Lopez, J. J. Carbo, J. M. Poblet, J. R. Galan-Mascaros, *Nat Chem* **2018**, *10*, 24-30.

[2] a) A. Bijelic, M. Aureliano, A. Rompel, *Angew Chem Int Edit* **2019**, *58*, 2980-2999; b) N. Gao, Z. Du, Y. Guan, K. Dong, J. Ren, X. Qu, *J Am Chem Soc* **2019**, *141*, 6915-6921.

[3] J. J. Chen, M. D. Symes, L. Cronin, *Nat Chem* **2018**, *10*, 1042-1047.

[4] a) M. J. Turo, L. F. Chen, C. E. Moore, A. M. Schimpf, *J Am Chem Soc* **2019**, *141*, 4553-4557; b) B. Nohra, H. El Moll, L. M. R. Albelo, P. Mialane, J. Marrot, C. Mellot-Draznieks, M. O'Keeffe, R. N. Biboum, J. Lemaire, B. Keita, L. Nadjo, A. Dolbecq, *J Am Chem Soc* **2011**, *133*, 13363-13374.

[5] a) L. B. Fullmer, R. H. Mansergh, L. N. Zakharov, D. A. Keszler, M. Nyman, *Cryst Growth Des* **2015**, *15*, 3885-3892; b) A. Llordes, G. Garcia, J. Gazquez, D. J. Milliron, *Nature* **2013**, *500*, 323-+.

[6] A. Muller, E. Beckmann, H. Bogge, M. Schmidtmann, A. Dress, *Angew Chem Int Edit* **2002**, *41*, 1162-+.

[7] A. Muller, S. Q. N. Shah, H. Bogge, M. Schmidtmann, *Nature* **1999**, *397*, 48-50.

[8] A. Muller, E. Krickemeyer, H. Bogge, M. Schmidtmann, C. Beugholt, P. Kogerler, C. Z. Lu, *Angew Chem Int Edit* **1998**, *37*, 1220-1223.

[9] X. K. Fang, P. Kogerler, Y. Furukawa, M. Speldrich, M. Luban, *Angew Chem Int Edit* **2011**, *50*, 5212-5216.

[10] A. R. de la Oliva, V. Sans, H. N. Miras, J. Yan, H. Y. Zang, C. J. Richmond, D. L. Long, L. Cronin, *Angew Chem Int Edit* **2012**, *51*, 12759-12762.

[11] K. Wassermann, M. H. Dickman, M. T. Pope, *Angewandte Chemie-International Edition in English* **1997**, *36*, 1445-1448.

[12] a) J. Y. Niu, P. T. Ma, H. Y. Niu, J. Li, J. W. Zhao, Y. Song, J. P. Wang, *Chem-Eur J* **2007**, *13*, 8739-8748; b) P. Huang, C. Qin, Z. M. Su, Y. Xing, X. L. Wang, K. Z. Shao, Y. Q. Lan, E. B. Wang, *J Am Chem Soc* **2012**, *134*, 14004-14010; c) J. P. Wang, H. Y. Niu, J. Y. Niu, *J Chem Sci* **2008**, *120*, 309-313; d) R. P. Bontchev, M. Nyman, *Angew Chem Int Edit* **2006**, *45*, 6670-6672.

[13] L. Jin, Z. K. Zhu, Y. L. Wu, Y. J. Qi, X. X. Li, S. T. Zheng, *Angew Chem Int Edit* **2017**, *56*, 16288-16292.

[14] Y. L. Wu, X. X. Li, Y. J. Qi, H. Yu, L. Jin, S. T. Zheng, *Angew Chem Int Edit* **2018**, *57*, 8572-8576.

[15] M. Nyman, F. Bonhomme, T. M. Alam, M. A. Rodriguez, B. R. Cherry, J. L. Krumhansl, T. M. Nenoff, A. M. Sattler, *Science* **2002**, *297*, 996-998.

[16] Z. W. Guo, Y. Chen, D. Zhao, Y. L. Wu, L. D. Lin, S. T. Zheng, *Inorg Chem* **2019**, *58*, 4055-4058.

[17] S. M. Chen, P. T. Ma, H. H. Luo, Y. Y. Wang, J. Y. Niu, J. P. Wang, *Chem Commun* **2017**, *53*, 3709-3712.

[18] a) J. H. Son, C. A. Ohlin, W. H. Casey, *Dalton T* **2012**, *41*, 12674-12677; b) J. H. Son, J. R. Wang, W. H. Casey, *Dalton T* **2014**, *43*, 17928-17933; c) C. A. Ohlin, E. M. Villa, J. C. Fettinger, W. H. Casey, *Dalton T* **2009**, 2677-2678; d) J. Y. Niu, F. Li, J. W. Zhao, P. T. Ma, D. D. Zhang, B. Bassil, U. Kortz, J. P. Wang, *Chem-Eur J* **2014**, *20*, 9852-9857.

[19] a) J. H. Son, D. H. Park, D. A. Keszler, W. H. Casey, *Chem-Eur J* **2015**, *21*, 6727-6731; b) Q. H. Geng, Q. S. Liu, P. T. Ma, J. P. Wang, J. Y. Niu, *Dalton Transac* **2014**, *43*, 9843-9846.

[20] D. Sures, M. Segado, C. Bo, M. Nyman, *J Am Chem Soc* **2018**, *140*, 10803-10813.

[21] M. Nyman, M. A. Rodriguez, C. F. Campana, *Inorg Chem* **2010**, *49*, 7748-7755.

[22] a) H. T. Evans, B. M. Gatehouse, *J Chem Soc Dalton* **1975**, 505-514; b) H. T. Evans, O. W. Rollins, *Acta Crystallogr B* **1976**, *32*, 1565-1567; c) B. Krebs, I. Paulatboschen, *Acta Crystallogr B* **1982**, *38*, 1710-1718.

[23] a) T. M. Alam, Z. L. Liao, L. N. Zakharov, M. Nyman, *Chem-Eur J* **2014**, *20*, 8302-8307; b) T. M. Anderson, S. G. Thoma, F. Bonhomme, M. A. Rodriguez, H. Park, J. B. Parise, T. M. Alam, J. P. Larentzos, M. Nyman, *Cryst Growth Des* **2007**, *7*, 719-723; c) P. C. Burns, K. A. Kubatko, G. Sigmon, B. J. Fryer, J. E. Gagnon, M. R. Antonio, L. Soderholm, *Angew Chem Int Edit* **2005**, *44*, 2135-2139.

[24] P. A. Abramov, C. Vicent, N. B. Kompankov, A. L. Gushchin, M. N. Sokolov, *Chem Commun* **2015**, *51*, 4021-4023.

[25] a) E. M. Villa, C. A. Ohlin, E. Balough, T. M. Anderson, M. D. Nyman, W. H. Casey, *Angew Chem Int Edit* **2008**, *26*, 4844-4846; b) M. Nyman, T. M. Alam, F. Bonhomme, M. A. Rodriguez, C. S. Frazer, M. E. Welk, *J Cluster Sci* **2006**, 2, 197-219; c) J. R. Black, M. Nyman, W. H. Casey, *J Am Chem Soc* **2006**, 45, 14712-14740.

[26] M. Nyman, P. C. Burns, *Chem Soc Rev* **2012**, *41*, 7354-7367.

Entry for the Table of Contents (Please choose one layout)

Layout 2:

COMMUNICATION

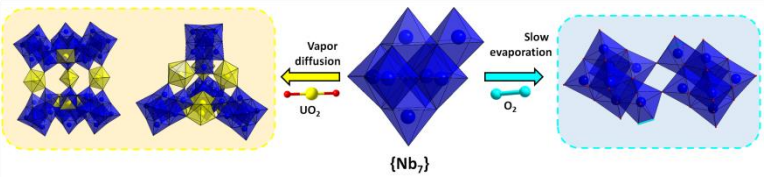

Nimble niobates. Nb-polyoxometalate (POM) chemistry lacks reactive building units that we can rationally manipulate. We devised a route to generate metastable heptaniobate building units *in-situ,* and captured them in three structures. The inert uranyl moiety harnesses heptaniobate in two structures, and peroxide stabilizes a third structure. This strategy provides a path to intricate architectures already demonstrated in Mo and W POMs.

Nicolas P. Martin[a], Enric Petrus[b], Mireia Segado[b], Ana Arteaga[a], Lev N. Zakharov[a], Carles Bo[b] and May Nyman[a]*

Page No. – Page No.

Strategic capture of the {Nb_7} polyoxometalate